Spin Injection and Nonlocal Spin Transport in Magnetic Nanostructures

S. Takahashi and S. Maekawa
Institute for Materials Research, Tohoku University, Sendai 980-8577, Japan,
and CREST, Japan Science and Technology Corporation, Kawaguchi 332-0012, Japan
(Dated: September 1, 2005)

We theoretically study the nonlocal spin transport in a device consisting of a nonmagnetic metal (N) and ferromagnetic injector (F1) and detector (F2) electrodes connected to N. We solve the spin-dependent transport equations in a device with arbitrary interface resistance from a metallic-contact to tunneling regime, and obtain the conditions for efficient spin injection, accumulation, and transport in the device. In a device containing a superconductor (F1/S/F2), the effect of superconductivity on the spin transport is investigated. The spin-current induced spin Hall effect in nonmagnetic metals is also discussed.

PACS numbers:

1. Introduction

There has been considerable interest in spin transport in magnetic nanostructures, because of their potential applications as spin-electronic devices [1]. The spin polarized electrons injected from a ferromagnet (F) into a nonmagnetic material (N) such as a normal metal, semiconductor, and superconductor create a nonequilibrium spin accumulation in N. The efficient spin injection, accumulation, and transport are central issues for utilizing the spin degree of freedom as in spin-electronic devices. It has been demonstrated that the injected spins penetrate into N over the spin-diffusion length ($l_{\rm N}$) of the order of $1\,\mu$m using spin injection and detection technique in F1/N/F2 trilayer structures (F1 is an injector and F2 a detector) [2]. Recently, several groups have succeeded in observing spin accumulation by the *nonlocal* spin injection and detection technique [3, 4, 5, 6, 7, 8, 9].

In this paper, we study the spin accumulation and spin current, and their detection in the nonlocal geometry of a F1/N/F2 nanostructure. We solve the diffusive transport equations for the electrochemical potential (ECP) for up and down spins in the structure of arbitrary interface resistances ranging from a metallic-contact to a tunneling regime, and examine the optimal conditions for spin accumulation and spin current. Efficient spin injection and detection are achieved when a tunnel barrier is inserted at the interface, whereas a large spin-current injection from N into F2 is realized when N is in metallic contact with F2, because F2 plays the role of strong spin absorber. In a tunnel device containing a superconductor (F1/S/F2), the effect of superconductivity on the spin transport is discussed. The spin-current induced anomalous Hall effect is also discussed.

2. Spin injection and accumulation

We consider a spin injection and detection device consisting of a nonmagnetic metal N connected to ferromagnetic injector F1 and detector F2 as shown in Fig. 1. The F1 and F2 are the same ferromagnets of width $w_{\rm F}$ and thickness $d_{\rm F}$ and are separated by distance L, and N of of width $w_{\rm N}$ and thickness $d_{\rm N}$. The magnetizations of F1 and F2 are aligned either parallel or antiparallel.

In the diffusive spin transport, the current $\mathbf{j}^\sigma$ for spin channel σ in the electrodes is driven by the gradient of ECP (μ^σ) according to $\mathbf{j}^\sigma = -(1/e\rho^\sigma)\nabla\mu^\sigma$, where ρ^σ is the resistivity. The continuity equations for the charge and spin curents in a steady state yield [2, 11, 12, 13, 14]

$$\nabla^2\left(\mu^\uparrow/\rho^\uparrow + \mu^\downarrow/\rho^\downarrow\right) = 0, \qquad (1)$$

$$\nabla^2\left(\mu^\uparrow - \mu^\downarrow\right) = l^{-2}\left(\mu^\uparrow - \mu^\downarrow\right), \qquad (2)$$

where l is the spin-diffusion length and takes $l_{\rm N}$ in N and $l_{\rm F}$ in F. We note that $l_{\rm N}$ ($l_{\rm Cu} \sim 1\mu$m [3], $l_{\rm Al} \sim 1\mu$m [2, 4]) is much larger than $l_{\rm F}$ ($l_{\rm Py} \sim 5\,$nm, $l_{\rm CoFe} \sim 12\,$nm, $l_{\rm Co} \sim 50\,$nm) [15].

We employ a simple model for the interfacial current across the junctions [11]. Due to the spin-dependent interface resistance R_i^σ ($i = 1, 2$), the ECP is discontinuous at the interface, and the current I_i^σ across the interface

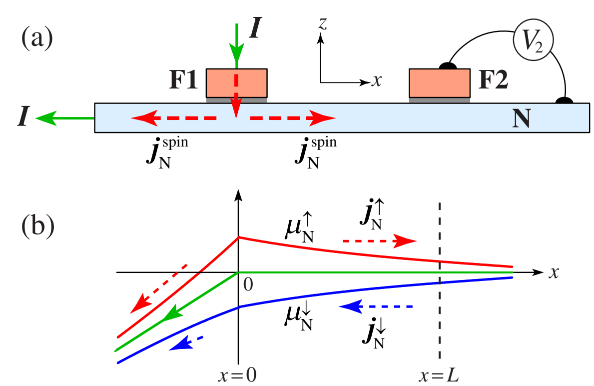

FIG. 1: (a) Spin injection and detection device (side view). The current I is applied from F1 to the left side of N. The spin accumulation at $x = L$ is detected by measuring voltage V_2 between F2 and N. (b) Spatial variation of the electrochemical potential (ECP) for up and down spin electrons in N.

$(z=0)$ is given by $I_i^\sigma = (1/eR_i^\sigma)\left(\mu_{\rm F}^\sigma|_{z=0^+} - \mu_{\rm N}^\sigma|_{z=0^-}\right)$, where the current distribution is assumed to be uniform over the contact area [16, 17]. In a transparent contact (tunnel junction) the discontinuous drop in ECP is much smaller (larger) than the spin splitting of ECP. The interfacial charge and spin currents are $I_i = I_i^\uparrow + I_i^\downarrow$ and $I_i^{\rm spin} = I_i^\uparrow - I_i^\downarrow$.

When the bias current I flows from F1 to the left side of N ($I_1 = I$), there is no charge current on the right side ($I_2 = 0$). The solution for Eqs. (1) and (2) takes the form $\mu_{\rm N}^\sigma(x) = \bar{\mu_{\rm N}} + \sigma\delta\mu_{\rm N}$ with the average $\bar{\mu_{\rm N}} = -(eI\rho_{\rm N}/A_{\rm N})x$ for $x<0$ and $\bar{\mu_{\rm N}} = 0$ for $x>0$, and the splitting $\delta\mu_{\rm N} = a_1 e^{-|x|/l_{\rm N}} - a_2 e^{-|x-L|/l_{\rm N}}$, where the a_1-term represents the spin accumulation due to spin injection at $x = 0$, while the a_2-term the decrease of spin accumulation due to the contact of F2. Note that the pure spin current $I_{\rm N}^{\rm spin} = I_{\rm N}^\uparrow - I_{\rm N}^\downarrow$ flows in the region of $x > 0$.

In the F1 and F2 electrodes, the solution takes the form $\mu_{{\rm F}i}^\sigma(z) = \bar{\mu_{{\rm F}i}} + \sigma b_i\,(\rho_{\rm F}^\sigma/\rho_{\rm F})\,e^{-z/l_{\rm F}}$, with $\bar{\mu}_{\rm F1} = -(eI\rho_{\rm F}/A_{\rm J})z + eV_1$ in F1 and $\bar{\mu}_{F2} = eV_2$ in F2, where V_1 and V_2 are the voltage drops across junctions 1 and 2, and $A_{\rm J} = w_{\rm N}w_{\rm F}$ is the contact area of the junctions.

Using the matching condition for the spin current at the interfaces, we can determine the constants a_i, b_i, and V_i. The spin-dependent voltages detected by F2 are $V_2^{\rm P}$ and $V_2^{\rm AP}$ for the parallel (P) and antiparallel (AP) alignment of magnetizations. The spin accumulation signal detected by F2, $R_s = (V_2^{\rm P} - V_2^{\rm AP})/I$, is given by [14]

$$R_s = 4R_{\rm N}\frac{\left(\dfrac{P_1}{1-P_1^2}\dfrac{R_1}{R_{\rm N}} + \dfrac{p_{\rm F}}{1-p_{\rm F}^2}\dfrac{R_{\rm F}}{R_{\rm N}}\right)\left(\dfrac{P_2}{1-P_2^2}\dfrac{R_2}{R_{\rm N}} + \dfrac{p_{\rm F}}{1-p_{\rm F}^2}\dfrac{R_{\rm F}}{R_{\rm N}}\right)e^{-L/l_{\rm N}}}{\left(1+\dfrac{2}{1-P_1^2}\dfrac{R_1}{R_{\rm N}} + \dfrac{2}{1-p_{\rm F}^2}\dfrac{R_{\rm F}}{R_{\rm N}}\right)\left(1+\dfrac{2}{1-P_2^2}\dfrac{R_2}{R_{\rm N}} + \dfrac{2}{1-p_{\rm F}^2}\dfrac{R_{\rm F}}{R_{\rm N}}\right) - e^{-2L/l_{\rm N}}}, \quad (3)$$

where $R_{\rm N} = \rho_{\rm N}l_{\rm N}/A_{\rm N}$ and $R_{\rm F} = \rho_{\rm F}l_{\rm F}/A_{\rm J}$ are the *spin-accumulation resistances* of the N and F electrodes, $A_{\rm N} = w_{\rm N}d_{\rm N}$ is the cross-sectional area of N, $R_i = R_i^\uparrow + R_i^\downarrow$ is the interface resistance of junction i, $P_i = |R_i^\uparrow - R_i^\downarrow|/R_i$ is the interfacial current spin-polarization, and $p_{\rm F} = |\rho_{\rm F}^\uparrow - \rho_{\rm F}^\downarrow|/\rho_{\rm F}$ is the spin-polarization of F. In metallic contact junctions, the spin polarizations, P_i and $p_{\rm F}$, range around 40–70% from GMR experiments [15] and point-contact Andreev-reflection experiments [18], whereas in tunnel junctions, P_i r anges around 30–55% from superconducting tunneling spectroscopy experiments with alumina tunnel barriers [19, 20, 21], and $\sim 85\,\%$ in MgO barriers [22, 23].

The spin accumulation signal R_s strongly depends on whether each junction is either a metallic contact or a tunnel junction. By noting that there is large disparity between $R_{\rm N}$ and $R_{\rm F}$ ($R_{\rm F}/R_{\rm N} \sim 0.01$ for Cu and Py [3]), we have the following limiting cases. When both junctions are transparent contact ($R_1, R_2 \ll R_{\rm F}$), we have [3, 12, 13]

$$R_s/R_{\rm N} = \frac{2p_{\rm F}^2}{(1-p_{\rm F}^2)^2}\left(\frac{R_{\rm F}}{R_{\rm N}}\right)^2 \sinh^{-1}(L/l_{\rm N}). \quad (4)$$

When junction 1 is a tunnel junction and junction 2 is a transparent contact (*e.g.*, $R_2 \ll R_{\rm F} \ll R_{\rm N} \ll R_1$), we have [14]

$$R_s/R_{\rm N} = \frac{2p_{\rm F}P_1}{(1-p_{\rm F}^2)}\left(\frac{R_{\rm F}}{R_{\rm N}}\right)e^{-L/l_{\rm N}}. \quad (5)$$

When both junctions are tunnel junctions ($R_1, R_2 \gg R_{\rm N}$), we have [2, 4]

$$R_s/R_{\rm N} = P_1P_2e^{-L/l_{\rm N}}, \quad (6)$$

where $P_{\rm T} = P_1 = P_2$. Note that R_s in the above limiting cases is independent of R_i.

We compare our theoretical result to experimental data measured by several groups. Figure 2 shows the theoretical curves and the experimental data of R_s as a function of L. The solid curves are the values in a tunnel device, and the dashed curves are those in a

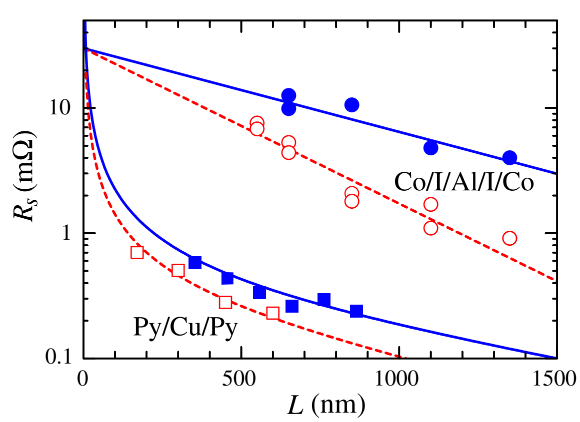

FIG. 2: Spin accumulation signal R_s as a function of distance L between the ferromagnetic electrodes in tunnel devices: (•, ∘) Co/I/Al/I/Co [4], and in metallic-contact devices: (□, ■) Py/Cu/Py [24, 25], where (•, ■) are the data at 4.2K and (∘, □) at room temperature.

metallic-contact device. We see that R_s in a metallic contact device is smaller by one order of magnitude than R_s in a tunnel device, because of the resistance mismatch ($R_{\rm F}/R_{\rm N} \ll 1$). Fitting Eq. (6) to the experimental data of Co/I/Al/I/Co (I$=$Al$_2$O$_3$) in Ref. [4] yields $l_{\rm N}$ = 650 nm (4.2 K), $l_{\rm N}$ = 350 nm (293 K), $P_1 = 0.1$, and $R_{\rm N} = 3\,\Omega$. Fitting Eq. (4) to the data of Py/Cu/Py in Ref. [24] at 4.2 K yields $l_{\rm N}$ = 920 nm, $R_{\rm N} = 5\,\Omega$, $[p_{\rm F}/(1-p_{\rm F}^2)](R_{\rm F}/R_{\rm N}) = 5\times10^{-3}$, and fitting to the data in Ref. [25] at 293 K yields $l_{\rm N}$ = 700 nm, $R_{\rm N} = 1.75\,\Omega$, and $[p_{\rm F}/(1-p_{\rm F}^2)](R_{\rm F}/R_{\rm N}) = 8\times10^{-3}$.

The spin splitting in N in the tunneling case is

$$2\delta\mu_{\rm N}(x) = P_1 e R_{\rm N} I e^{-|x|/l_{\rm N}}. \tag{7}$$

In the case of Co/I/Al/I/Co, $\delta\mu_{\rm N}(0) \sim 15\,\mu$V for $P_1 \sim 0.1$, $R_{\rm N} = 3\,\Omega$, and $I = 100\,\mu$A [4], which is much smaller than the superconducting gap $\Delta \sim 200\mu$eV of an Al film.

3. Nonlocal spin injection and manipulation

We next study how the spin-current flow in the structure is affected by the interface condition, especially, the spin current through the N/F2 interface, because of the interest in spin-current induced magnetization switching [26].

The spin current injected nonlocally across the N/F2 interface is given by [14]

$$I_{\rm N/F2}^{\rm spin} = 2I\frac{\left(\dfrac{P_1}{1-P_1^2}\dfrac{R_1}{R_{\rm N}} + \dfrac{p_{\rm F}}{1-p_{\rm F}^2}\dfrac{R_{\rm F}}{R_{\rm N}}\right)e^{-L/l_{\rm N}}}{\left(1+\dfrac{2}{1-P_1^2}\dfrac{R_1}{R_{\rm N}}+\dfrac{2}{1-p_{\rm F}^2}\dfrac{R_{\rm F}}{R_{\rm N}}\right)\left(1+\dfrac{2}{1-P_2^2}\dfrac{R_2}{R_{\rm N}}+\dfrac{2}{1-p_{\rm F}^2}\dfrac{R_{\rm F}}{R_{\rm N}}\right) - e^{-2L/l_{\rm N}}}. \tag{8}$$

A large spin-current injection occurs when junction 2 is a metallic contact ($R_2 \ll R_{\rm N}$) and junction 1 is a tunnel junction ($R_1 \gg R_{\rm N}$), yielding

$$I_{\rm N/F2}^{\rm spin} \approx P_1 I e^{-L/l_{\rm N}}, \tag{9}$$

for F2 with very short $l_{\rm F}$. The spin current flowing in N on the left side of F2 is $I_{\rm N}^{\rm spin} = P_1 I e^{-x/l_{\rm N}}$, which is two times larger than that in the absence of F2, while on the right side left $I_{\rm N}^{\rm spin} \approx 0$. This indicates that F2 like Py and CoFe works as a strong absorber (sink) for spin current, providing a method for magnetization reversal in nonlocal devices with reduced dimensions of F2 island [27].

4. Spin injection into superconductors

The spin transport in a device containing a superconductor (S) such as Co/I/Al/I/Co is of great interest, because R_s is strongly influenced by opening the superconducting gap. In such tunneling device, the spin signal would be strongly affected by opening the superconducting gap Δ.

We first show that the spin diffusion length in the superconducting state is the same as that in the normal state [28, 29]. This is intuitively understood as follows. Since the dispersion curve of the quasiparticle (QP) excitation energy is given by $E_k = \sqrt{\xi_k^2+\Delta^2}$ with one-electron energy ξ_k [30], the QP's velocity $\tilde{v}_k = (1/\hbar)(\partial E_k/\partial k) = (|\xi_k|/E_k)v_k$ is slower by the factor $|\xi_k|/E_k$ compared with the normal-state velocity $v_k(\approx v_F)$. By contrast, the impurity scattering time [31] $\tilde{\tau} = (E_k/|\xi_k|)\tau$ is longer by the inverse of the factor. Then, the spin-diffusion length in S, $l_{\rm S} = (\tilde{D}\tilde{\tau}_{sf})^{1/2}$ with $\tilde{D} = \frac{1}{3}\tilde{v}_k^2\tilde{\tau}_{\rm tr} = (|\xi_k|/E_k)D$ turns out to be the same as $l_{\rm N}$, owing to the cancellation of the factor $|\xi_k|/E_k$.

The spin accumulation in S is determined by balancing the spin injection rate with the spin-relaxation rate:

$$I_1^{\rm spin} - I_2^{\rm spin} + e\left(\partial S/\partial t\right)_{\rm sf} = 0, \tag{10}$$

where S is the total spins in S, and $I_1^{\rm spin}$ and $I_2^{\rm spin}$ are the rates of incoming and outgoing spin currents through junction 1 and 2, respectively. At low temperatures the spin relaxation is dominated by spin-flip scattering via the spin-orbit interaction $V_{\rm so}$ at nonmagnetic impurities or grain boundaries. The scattering matrix elements of $V_{\rm so}$ over QP states $|\mathbf{k}\sigma\rangle$ with momentum $\mathbf{k}$ and spin σ has the form: $\langle\mathbf{k}'\sigma'|V_{\rm so}|\mathbf{k}\sigma\rangle = i\eta_{\rm so}\left(u_{k'}u_k - v_{k'}v_k\right)[\vec{\sigma}_{\sigma'\sigma}\cdot(\mathbf{k}\times\mathbf{k}')/k_{\rm F}^2]V_{\rm imp}$, where $\eta_{\rm so}$ is the spin-orbit coupling parameter, $V_{\rm imp}$ is the impurity potential, σ is the Pauli spin matrix, and $u_k^2 = 1-v_k^2 = \frac{1}{2}\left(1+\xi_k/E_k\right)$ are the coherent factors [30]. Using the golden rule for spin-flip scattering processes, we obtain the spin-relaxation rate in the form [32, 33]

$$\left(\partial S/\partial t\right)_{\rm sf} = -S/\tau_{\rm sf}(T), \tag{11}$$

where $S = \chi_s(T)S_N$ with S_N the normal-state value and $\chi_s(T)$ the QP spin-susceptibility called the Yosida func-

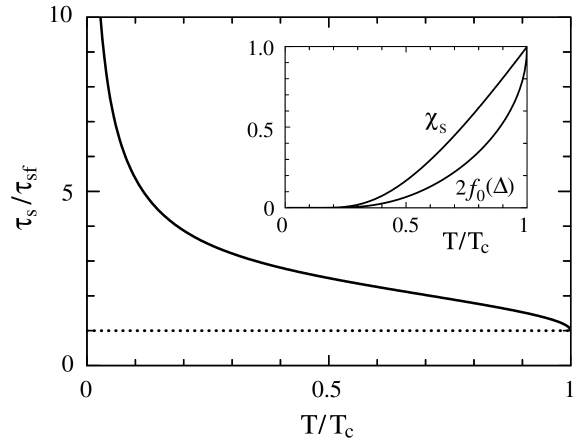

FIG. 3: Temperature dependence of the spin relaxation time τ_s in the superconducting state. The inset shows χ_s and $2f_0(\Delta)$ vs. T.

tion [34], and

$$\tau_s(T) = [\chi_s(T)/2f_0(\Delta)]\,\tau_{\rm sf}, \tag{12}$$

where $\tau_{\rm sf}$ is the spin-flip scattering time in the normal state. Equation (12) was derived earlier by Yafet [33] who studied the electron-spin resonance (ESR) in the superconducting state. Figure 3 shows the temperature dependence of $\tau_s/\tau_{\rm sf}$. In the superconducting state below the superconducting critical temperature T_c, τ_s becomes longer with decreasing T according to $\tau_s \simeq (\pi\Delta/2k_{\rm B}T)^{1/2}\tau_{\rm sf}$ at low temperatures.

Since the spin diffusion length in the superconducting state is the same as that in the normal state, the ECP shift in S is $\delta\mu_{\rm S} = \left(\tilde{a}_1 e^{-|x|/l_{\rm N}} - \tilde{a}_2 e^{-|x-L|/l_{\rm N}}\right)$, where $\tilde{a}_i$ is calculated as follows. In the tunnel device, the tunnel spin currents are $I_1^{\rm spin} = P_1 I$ and $I_2^{\rm spin} \approx 0$, so that Eqs (10) and (11) give the coefficients $\tilde{a}_1 = P_1 R_{\rm N} eI/[2f_0(\Delta)]$ and $\tilde{a}_2 \approx 0$, leading to the spin splitting of ECP in the superconducting state [14]

$$\delta\mu_{\rm S}(x) = \frac{1}{2}P_1\frac{R_{\rm N}eI}{2f_0(\Delta)}e^{-|x|/l_{\rm N}}, \tag{13}$$

indicating that the splitting in ECP is enhanced by the factor $1/[2f_0(\Delta)]$ compared with the normal-state value (see Eq. 7). The detected voltage V_2 by F2 at distance L is given by $V_2 = \pm P_2\delta\mu_{\rm S}(L)$ for the P (+) and AP (−) alignments. Therefore, the spin signal R_s in the superconducting state becomes [14]

$$R_s = P_1P_2R_{\rm N}e^{-L/l_{\rm N}}/[2f_0(\Delta)]. \tag{14}$$

The above result is also obtained by the replacement $\rho_{\rm N} \to \rho_{\rm N}/[2f_0(\Delta)]$ in the normal-state result of Eq. (6), which results from the fact that the QP carrier density decreases in proportion to $2f_0(\Delta)$, and superconductors become a low carrier system for spin transport. The rapid increase in R_s below T_c reflects the strong reduction of the carrier population. However, when the splitting $\delta\mu_{\rm S} \sim \frac{1}{2}eP_1R_{\rm N}I/[2f(\Delta)]$ at $x=0$ becomes comparable to or larger than Δ, the superconductivity is suppressed or destroyed by pair breaking due to the spin splitting [35, 36, 37, 38, 39, 40]. This prediction can be tested by measuring R_s in Co/I/Al/I/Co or Py/I/Al/I/Py in the superconducting state.

5. Spin-current induced spin Hall effect

The basic mechanism for the spin Hall effect (SHE) is the spin-orbit interaction in N, which causes a spin-asymmetry in the scattering of conduction electrons by impurities; up-spin electrons are preferentially scattered in one direction and down-spin electrons in the opposite direction. Spin injection techniques makes it possible to cause SHE in *nonmagnetic* conductors. When spin-polarized electrons are injected from a ferromagnet (F) to a nonmagnetic electrode (N), these electrons moving in N are deflected by the spin-orbit interaction to induce the Hall current in the transverse direction and accumulate charge on the sides of N [41, 42, 43].

We consider a spin-injection Hall device shown in Fig. 4. The magnetization of F electrode points to the z direction. Using the Boltzmann transport equation which incorporates the asymmetric scattering by nonmagnetic impurities, we obtain the total charge current in N [43]

$$\mathbf{j}_{\rm tot} = \alpha_{\rm H}\,[\hat{\mathbf{z}} \times \mathbf{j}_{\rm spin}] + \sigma_{\rm N}\mathbf{E}, \tag{15}$$

where the first term is the Hall current $\mathbf{j}_{\rm H}$ induced by the spin current, the second term is the Ohmic current, $\mathbf{E}$ is the electric field induced by surface charge, and $\alpha_{\rm H} \sim \eta_{\rm so}N(0)V_{\rm imp}$ (skew scattering). In the open circuit condition in the transverse direction, the y component of $\mathbf{j}_{\rm tot}$ vanishes, so that the nonlocal Hall resistance

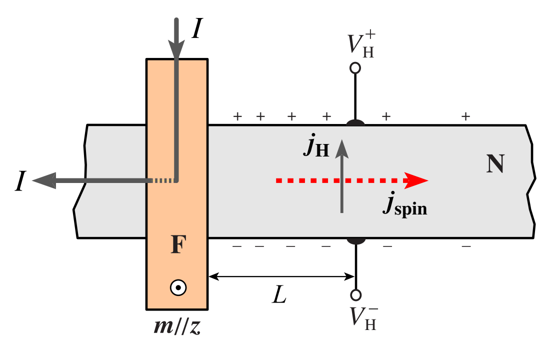

FIG. 4: Spin injection Hall device (top view). The magnetic moment of F is aligned perpendicular to the plane. The anomalous Hall voltage $V_{\rm H} = V_{\rm H}^+ - V_{\rm H}^-$ is induced in the transverse direction by injection of spin-polarized current.

TABLE I: Spin-orbit coupling parameter of Cu and Al.

	$l_{\rm N}$ (nm)	$\rho_{\rm N}$ ($\mu\Omega$cm)	$\tau_{\rm imp}/\tau_{\rm sf}$	$\eta_{\rm so}$
Cu	1000[a]	1.43[a]	0.70×10^{-3}	0.040
Cu	546[b]	3.44[b]	0.41×10^{-3}	0.030
Al	650[c]	5.90[c]	0.36×10^{-4}	0.009
Al	705[d]	5.88[d]	0.30×10^{-4}	0.008
Ag	195[e]	3.50[e]	0.50×10^{-2}	0.110

[a]Ref. [3], [b]Ref. [8], [c]Ref. [4], [d]Ref. [45], [e]Ref. [10].

$R_{\rm H}=V_{\rm H}/I$ becomes

$$R_{\rm H}=\frac{1}{2}\left(P_1\alpha_{\rm H}\rho_{\rm N}/d_{\rm N}\right)e^{-L/l_{\rm N}}, \tag{16}$$

in the tunneling case. Recently, SHE induced by the spin-current have been measured in a Py/Cu structure using the spin injection technique [44, 45, 46].

It is noteworthy that the product $\rho_{\rm N}l_{\rm N}$ is related to the spin-orbit coupling parameter $\eta_{\rm so}$ as [48]

$$\rho_{\rm N}l_{\rm N}=\frac{\sqrt{3}\pi}{2}\frac{R_{\rm K}}{k_{\rm F}^2}\sqrt{\frac{\tau_{\rm sf}}{\tau_{\rm imp}}}=\frac{3\sqrt{3}\pi}{4}\frac{R_{\rm K}}{k_{\rm F}^2}\frac{1}{\eta_{\rm so}}, \tag{17}$$

where $R_{\rm K}=h/e^2\sim 25.8\,{\rm k}\Omega$ is the quantum resistance. The formula (17) provides a method for obtaining information for spin-orbit scattering in nonmagnetic metals. Using the experimental data of $\rho_{\rm N}$ and $l_{\rm N}$ and the Fermi momentum $k_{\rm F}$ [49] in Eq. (17), we obtain the value of the spin-orbit coupling parameter $\eta_{\rm so}=0.01$–0.04 in Cu and Al as listed in Table 1. Therefore, Eq. (16) yields $R_{\rm H}$ of the order of $1\,{\rm m}\Omega$, indicating that the spin-current induced SHE is observable by using the nonlocal geometry.

Acknowledgement

The authors thank M. Ichimura, H. Imamura, and T. Yamashita for valuable discussions. This work is supported by a Grant-in-Aid for Scientific Research from MEXT and the NAREGI Nanoscience Project.

[1] *Concept in Spin Electronics*, edited by S. Maekawa (Oxford Univ Press, 2006).
[2] M. Johnson and R.H. Silsbee, Phys. Rev. Lett. **55**, 1790 (1985); *ibid.* **60**, 377 (1988); M. Johnson, *ibid.* **70**, 2142 (1993).
[3] F. J. Jedema, A. T. Filip and B. J. van Wees, Nature (London) **410**, 345 (2001)
[4] F. J. Jedema, H. B. Heersche, A. T. Filip, J. J. A. Baselmans, and B. J. van Wees, Nature (London) **416**, 713 (2002).
[5] T. Kimura, J. Hamrle, Y. Otani, K. Tsukagoshi, and Y. Aoyagi, Appl. Phys. Lett. **85**, 3795 (2004); T. Kimura, J. Hamrle, Y. Otani, Phys. Rev. B **72**, 14461 (2005).
[6] M. Urech, J. Johansson, V. Korenivski and D. B. Haviland, J. Magn. Magn. Mater. **272-276**, E1469 (2004).
[7] Y. Ji, A. Hoffmann, J. S. Jiang, and S. D. Bader, Appl. Phys. Lett. **85**, 6218 (2004).
[8] S. Garzon, I. Žutić, and R. A. Webb, Phys. Rev. Lett. **94**, 176601 (2005).
[9] K. Miura, T. Ono, S. Nasu, T. Okuno, K. Mibu, and T. Shinjo, J. Magn. Magn. Mater. **286**, 142 (2005).
[10] R. Godfrey and M. Johnson, Phys. Rev. Lett. **96** (2006) 136601.
[11] T. Valet and A. Fert, Phys. Rev. B **48**, 7099 (1993).
[12] A. Fert and S.F. Lee, Phys. Rev. B **53**, 6554 (1996).
[13] S. Hershfield and H.L. Zhao, Phys. Rev. B **56**, 3296 (1997).
[14] S. Takahashi and S. Maekawa, Phys. Rev. B **67**, 052409 (2003).
[15] J. Bass and W.P. Pratt Jr., J. Magn. and Magn. Mater. **200** (1999) 274.
[16] M. Ichimura, S. Takahashi, K. Ito, and S. Maekawa, J. Appl. Phys. **95**, 7225 (2004).
[17] J. Hamrle, T. Kimura, T. Yang, and Y. Otani, Phys. Rev. B **71**, 094434 (2005).
[18] R. J. Soulen Jr. *et al.*, Science **282**, 85 (1998).
[19] R. Meservey and P. M. Tedrow, Phys. Rep. **238**, 173 (1994).
[20] J. S. Moodera and G. Mathon, J. Magn. Magn. Mater. **200**, 248 (1999).
[21] D. J. Monsma and S. S. P. Parkin, Appl. Phys. Lett. **77**, 720 (2000).
[22] S. S. P. Parkin *et al* Nature Materials **3**, 862 (2004).
[23] S. Yuasa, T. Nagahama, A. Fukushima, Y. Suzuki, and K. Ando, Nature Materials **3**, 868 (2004).
[24] S. Garzon, Ph.D. Thesis (Univ. Maryland, 2005).
[25] T. Kimura, J. Hamrle, and Y. Otani, J. Magn. Soc. Jpn. **29**, 192 (2005).
[26] J. C. Slonczewski, J. Mag. Mag. Mater. **159**, L1 (1996).
[27] T. Kimura, Y. Otani, and J. Hamrle, Phys. Re. Lett. **96**, 037201 (2006). In their device of Py/Cu/Py, the junctions are both metallic contact, so that $I^{\rm spin}_{\rm N/F2}\approx[p_{\rm F}/(1-p_{\rm F}^2)]I(R_{\rm F}/R_{\rm N})\sinh^{-1}(L/l_{\rm N})$.
[28] T. Yamashita, S. Takahashi, H. Imamura, and S. Maekawa, Phys. Rev. B **65**, 172509 (2002).
[29] J. P. Morten, A. Brataas, and W. Belzig [Phys. Rev. B **70**, 212508 (2004)] have pointed out that, in the *elastic* transport regime, the spin-diffusion length is renormalized in the superconducting state.
[30] M. Tinkham, *Introduction to Superconductivity* (McGraw-Hill, New York, 1996).
[31] J. Bardeen, G. Rickayzen, and L. Tewordt, Phys. Rev. **113**, 982 (1959).
[32] S. Takahashi, T. Yamashita, H. Imamura, S. Maekawa, J. Magn. Magn. Mater. **240**, 100 (2002).
[33] Y. Yafet, Phys. Lett. **98**, 287 (1983).
[34] K. Yosida, Phys. Rev. **110**, 769 (1958).
[35] S. Takahashi, H. Imamura, and S. Maekawa, Phys. Rev. Lett. **82**, 3911 (1999).
[36] S. Takahashi, H. Imamura, and S. Maekawa, J. Appl. Phys. **85**, 5227 (2000); Physica C **341-348**, 1515 (2000).
[37] C. D. Chen, Watson Kuo, D. S. Chung, J. H. Shyu, and C. S. Wu, Phys. Rev. Lett. **88**, 047004 (2002).
[38] J. Johansson, M. Urech, D. Haviland, and V. Korenivski, J. Appl. Phys. **93**, 8650 (2003).
[39] D. Wang and J. G. Lu, J. Appl. Phys. **97**, 10A708 (2005).

[40] T. Daibou, M. Oogane, Y. Ando, and T. Miyazaki, (unpublished).
[41] J. E. Hirsch, Phys. Rev. Lett. **83** (1999) 1834.
[42] S. Zhang, Phys. Rev. Lett. **85** (2001) 393.
[43] S. Takahashi and S. Maekawa, Phys. Rev. Lett. **88**, 116601 (2002).
[44] T. Kimura, Y. Otani, K. Tsukagoshi and Y. Aoyagi, J. Magn. Magn. Mater. **272-276**, e1333 (2004).
[45] S. O. Valenzuela and M. Tinkham, Nature **442**, 176 (2006).
[46] T. Kimura, Y. Otani, T. Sato, S. Takahashi, and S. Maekawa, cond-mat/0609304.
[47] F. J. Jedema, M. S. Nijboer, A. T. Filip, and B. J. van Wees, Phys. Rev. B **67**, 085319 (2003).
[48] S. Takahashi, H. Imamura, and S. Maekawa, Chapter 8 in *Concept in Spin Electronics*, edited by S. Maekawa (Oxford Univ Press, 2006).
[49] N. W. Ashcroft and D. Mermin, *Solid State Physics*, (Saunders College, 1976).